Pergamon

0301-9322(94)00076-X

Int. J. Multiphase Flow Vol. 21, No. 3, pp. 405–418, 1995

0301-9322/95 $9.50 + 0.00

EXPERIMENTAL STUDY OF THE TWO-PHASE FLOW DYNAMICS IN NUCLEATE AND FILM POOL BOILING

P. M. CARRICA, S. A. LEONARDI and A. CLAUSSE
Centro Atómico Bariloche and Instituto Balseiro, 8400-Bariloche, Argentina

(Received 24 June 1993; in revised form 12 October 1994)

Abstract—An experimental study is conducted to measure the transient characteristics of the local boiling process close to the heated wall. Nucleate and film boiling two-phase parameters were measured for power oscillations in a small horizontal heater immersed in stagnant liquid. A method for measuring fast temporal variations of void fraction and the interfacial impact rate is presented. Ensemble averages of the data have been carried out to obtain time evolution of the void fraction and the interfacial impact rate at the probe tip. R-113, R-11 and water have been used as working fluids, finding important differences between the behavior of the freons and water at the boiling crises. The critical heat flux in freons is associated with a sudden transition in the impact rate and the void fraction, which supports the theory of hydrodynamic instability. On the other hand, the experiments in water suggest the existence of two transitions: a hydrodynamic transition from bubbling regime to "mushroom" regime followed by a liquid film dryout type of CHF, in agreement with the theory of Haramura & Katto.

Key Words: boiling, void fraction, critical heat flux

INTRODUCTION

Boiling heat transfer has been the subject of extensive studies over the past several decades due to its effective heat transfer characteristics. Although numerous studies of boiling are available in the literature, an understanding of the basic mechanisms involved in boiling phenomena has not reached a comparable development to the present (Lienhard 1988). The main reason for the limited success of the attempts to describe nucleate and film boiling processes in a mechanistic way is the lack of understanding of the interaction of the several surface and fluid parameters.

Considerable effort has been made to study the relation between heat flux and the difference between the liquid bulk temperature and the heater wall temperature in boiling. For almost every surface condition the wall temperature is essentially constant in nucleate boiling (Van Stralen & Cole 1979), and this assumption is good enough for most of the applications. This almost isothermal behavior of nucleate boiling has led many investigators to postulate hydrodynamic mechanisms (Zuber 1959; Haramura & Katto 1983) for nucleate boiling crisis or critical heat flux (CHF). Recently several physics based models have been presented which represents the valuable efforts made towards a more fundamental understanding of the complex process of boiling (Carrica & Clausse 1992; Dhir & Liaw 1989). A good review of recent developments can be found in Dhir (1991).

Very little work has been done to study the two-phase flow near the heater wall, although much information can be obtained to understand the basic phenomena of boiling. Liaw & Dhir (1989) measured the void fraction variations with the distance from a vertical heater in water, using the gamma ray attenuation technique. They found that for high heat fluxes the void fraction presents a peak near the heater wall. Similar trends were measured for horizontal heaters in FC-72 (Bonetto *et al.* 1995) and water (Carrica *et al.* 1992; Iida & Kobayasi 1969), using local phase detection probes. Transition and film boiling are not as studied as nucleate boiling, but good reviews are available from Kalinin *et al.* (1975, 1987). A recent paper by Shoji (1992) deals with the same problem in boiling water including the transition and film boiling regimes. To our knowledge there is no other extensive experimental work dealing with the problem of the two-phase flow near the heater wall in these boiling regimes.

In this work an experimental study is conducted to measure the transient characteristics of the local boiling process close to the heated wall. Both nucleate and film boiling two-phase parameters were measured for power oscillations in a small horizontal heater immersed in stagnant liquid.

Table 1. Some properties at normal pressure of the three fluids used in this work

Quantity	Units	R-113 ($C_2Cl_3F_3$)	R-11 (CCl_3F)	Water (H_2O)
Surface tension	kg/s^2	0.019	0.018	0.059
Vapor density	kg/m^3	7.38	5.86	0.6
Liquid density	kg/m^3	1565	1467	958
Vaporization latent heat	kJ/kg °C	147	180	2257
Saturation temperature	°C	47.6	23.6	100
Critical heat flux	W/cm^2	26	30	170
Leidenfrost heat flux	W/cm^2	8	11	60
Thermal conductivity	W/m °C	0.0658	0.0865	0.681
Liquid viscosity	(kg/m s) × 10^5	68	42	28.3

Using an ensemble average technique, local void fraction and interfacial impact rate during the power oscillations were calculated.

EXPERIMENTAL SET-UP

The experiments were carried out in three different fluids: water and freons R-113 and R-11. In table 1 the main physical and thermal properties of these fluids corresponding to saturation temperature at normal pressure are shown.

A diagram of the experimental apparatus is shown in figure 1. A stainless steel vessel 2000 cm^3 in volume was used for both R-113 and R-11 and a Pyrex glass vessel 3000 cm^3 in volume was used for water. The test section was placed inside the vessel containing liquid at saturation temperature. The liquid temperature was controlled using an external heater. The vapor generated at the test section was condensed back to the pool by means of a coiled heat exchanger. A small reflux condenser was used to ensure atmospheric pressure in the system and to minimize the vapor losses. Before the series of experiments the liquid was boiled for about 20 min for degassing.

The heater was a thin platinum foil of 5 mm × 10 mm × 25 μm attached to a mica substrate for downward thermal insulation. The contacts were made by means of copper electrodes pressing on the platinum foil. A contact resistance of 0.1 mΩ was measured, and the heater resistance at 20°C ranged from 25 to 30 mΩ in all the experiments. After about 1 h of heat dissipation in water the resistivity of the heater increased about 5%. When the resistivity changed more than this limit a

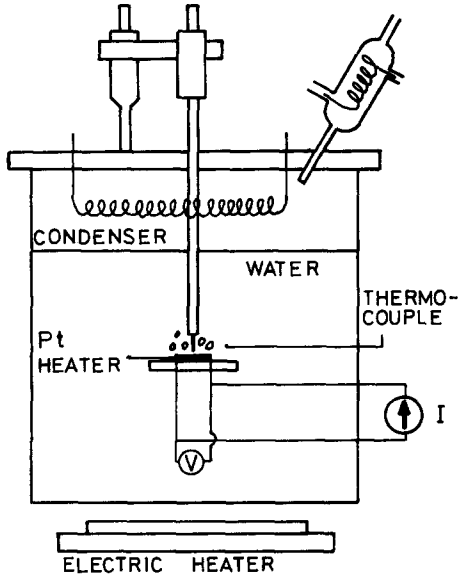

Figure 1. Experimental apparatus.

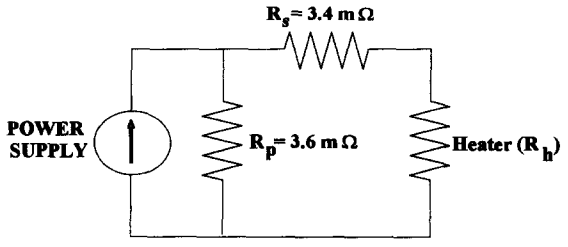

Figure 2. Electric circuit to supply power to the heater.

new heater was used. Prior to the measurements the heater was polished with #500 sandpaper. The heater was placed horizontally in the vessel, so as to ensure no side wall blockage or immersion depth effects.

The power to the heater was provided by a Bruker DC power supply. The electrical current was controlled by a PC-XT computer. A resistance parallel to the heater was added as shown in figure 2 to avoid heater burn-out when the transition from nucleate to film boiling occurs. The parallel resistance was maintained in a water bath in order to avoid possible resistivity changes due to temperature variations. In the transition from film to nucleate boiling in water the voltage in the heater changed about 10%.

Local phase detection probes

A local phase detection probe was located 2.5 mm above the center of the heater on the horizontal plane. The probe tip position was chosen to perform measurements out of the macrolayer and the vapor film in film boiling. Also above this position a maximum in the void fraction has been observed by many researchers as stated in the Introduction.

For the dielectric refrigerants R-113 and R-11 a sapphire prism tip (AID 1977) optical probe (RBI, type 7915) was used. After each set of experiments the probe tip was polished with diamond paste to remove the carbon depositions built up by freon decomposition at film boiling temperatures. Carbon depositions also appeared on the heater so it was polished with #500 sandpaper. Due to the need of cleaning the tip of the probe, the use of U-shaped or monofiber tip probes was avoided because of their great fragility (Cartellier & Achard 1991).

It was found that when using the sapphire optical probe in film boiling in water, light emissions from the hot spot were detected by the probe causing the signal to saturate. This effect gives non-realistic results. Synchronous detection (Annunziato *et al.* 1987) can be implemented to overcome this problem, but these methods have not been tested for the case of very intense light sources near the tip of the probe. Therefore, for the high working temperatures involved in film boiling in water a conductive probe was specifically designed (Carrica *et al.* 1993). The tip of the probe was made of steel wire 50 μm in diameter covered by a thin layer of Omega bond 200 high temperature insulator. The resulting diameter of the tip was 150 μm. Following the procedure of Van der Welle (1985), only the front end of the tip was uninsulated. A casing tube 2 mm in diameter was used as the second electrode, 80 kHz square wave excitation was used to avoid polarization and electrochemical attack. The rise time of the signal level in boiling water was about 0.5 ms.

The signal of the probe was digitalized to obtain the local phase indicator function:

$$X_G(x, t) = \begin{cases} 1 \text{ when gas is present at the probe tip} \\ 0 \text{ when liquid is present at the probe tip} \end{cases} \quad [1]$$

where X_G is the local phase indication function.

The phase indicator function was acquired with the computer through a specifically designed card. The minimum time between interfaces accepted by the acquisition system was 0.2 ms.

The digitalization of the probe signal was performed by means of a single threshold technique (Cartellier 1990), which was set to 75% for the optical probe in R-11 and R-13 to avoid the detection of neighboring bubbles (Galaup 1975), and 50% for the conductive probe in water. Probes were calibrated in an air–water section at different temperatures by setting the threshold, which matched the void fraction obtained by the gamma ray attenuation technique, with the corresponding one of the probes. Ideally, a direct calibration with the same system would be more appropriate, but unfortunately the liquid chordal length is excessively long compared with the thickness of the two-phase plume.

Experimental procedure

The electrical current generated by the power supply was controlled to describe a triangular power oscillation with frequencies of 0.5 and 0.05 Hz, according to the law:

$$I(t) = \begin{cases} I_{\max} \sqrt{2t/T}, & t < T/2 \\ I_{\max} \sqrt{2(T-t)/T}, & T/2 \leqslant t \leqslant T \end{cases} \quad [2]$$

where I is the electric current generated by the power supply and $T = 1/f$ is the period of the oscillation. These periods were chosen to study two cases:

(1) $T = 2$ s: the time constant of the thermal inertia of the heater is of the same order as the power oscillation period. In this case the effects of the thermal characteristics of the heater are of importance in the two-phase flow generated near the heater. As the measured time constant of the heater was about 0.5 s (see appendix), a period of 2 s was chosen.

(2) $T = 20$ s: the period is much higher than the thermal relaxation time of the heater. In this case the quasi-steady-state is observed.

The power to the heater is calculated according to the circuit of figure 2:

$$P_h = \frac{R_p^2 R_h I^2}{(R_s + R_p + R_h)^2} \quad [3]$$

where

P_h = power of heater
R_h = resistance of heater
R_p = resistance in parallel
R_s = resistance in series.

Combining [2] and [3] it can be seen that the heat flux increases linearly with time provided that the heater resistance remains constant, as approximately occurs in nucleate boiling. The oscillation amplitude was set in a range from zero to a maximum level set greater than the critical heat flux (CHF), as as to assure that the transitions from nucleate to film boiling, and vice versa, can be studied. The value of CHF was determined by observing sequences of power cycles of increasing amplitude, and observing the hot spot occurrence as well as measuring the heater temperature escalation.

The temperature of the heater at the transition from CHF to film boiling was about 1200°C in water, 500°C in R-11 and 450°C in R-113. These temperatures were calculated measuring the change in the heater resistivity. In water and R-11, the high temperatures constituted a limitant of the incursion into the film boiling regime, since there was a danger of too much freon decomposition and/or heater failure. Experiments were carried out for about 50 cycles at 0.05 Hz and 500 cycles at 0.5 Hz, and the phase indication function was recorded in magnetic media for off-line analysis.

Statistical ensemble averages of the data were performed dividing each of the N power cycles in k time intervals of duration T/k. Assuming that the system satisfies the ergodic hypothesis, ensemble averages of the void fraction and the interfacial impact rate at the probe for N identical experiments can be defined similarly to the mean quantitites in turbulence theory (Hinze 1975):

$$\epsilon_G(\mathbf{x}, t_i) = \sum_{j=1}^{N} \frac{k}{TN} \int_{t_i - k/2T}^{t_i + k/2T} X_j(x, t')\, dt' \quad [4]$$

$$\dot{n}(x, t_i) = \frac{1}{N} \sum_{j=1}^{N} \frac{k n_{ij}}{T} \quad [5]$$

Here ϵ_G is the void fraction averaged in the time interval centered in t_i, $\dot{n}$ is the interfacial impact rate at the tip of the probe and n_{ij} is the number of interfaces detected in the ith interval of the jth cycle. The total integration time in each interval is then NT/k. This number must be greater than 30 s to minimise statistical errors and obtain smooth curves.

The statistical errors of ϵ_G and $\dot{n}$ are calculated by:

$$E_\epsilon^i = \frac{\sqrt{\sum_{j=1}^{N} \epsilon_{G_{ij}}^2 - N\epsilon_{G_i}^2}}{N} \quad [6]$$

$$E_{\dot{n}}^{j} = \frac{\sqrt{\sum_{j=1}^{N} \dot{n}_{ij}^2 - N\dot{n}_i^2}}{N} \qquad [7]$$

Figure 3 shows graphically the way of performing the ensemble averages for N cycles. These cycles can be measured in different experimental runs with the only requirement that the experimental conditions must be exactly the same.

EXPERIMENTAL RESULTS

Experiments in R-113

Power cycles with current varying from 0 to 240 A were performed for both 0.5 and 0.05 Hz. The CHF occurs at $I = 195$ A, corresponding to a heat flux of 26 W/cm^2. The heater resistance was 22 mΩ. Five independent runs using the same heater were made for each frequency in order to verify repetitivity in the results. The latter supports the assumption that the data were not affected by the carbon depositions on the probes within the runs. Once the latter was checked the five experimental results were averaged. The ensemble averaging procedure was carried out using 100 time intervals in each case. This gives an effective integration time of about 50 s for each point.

Figure 4 shows the temporal evolution of the void fraction and the interfacial impact rate at the probe tip position for an oscillation of period $T = 20$ s. The onset of nucleate boiling is reached at 1 s and later the void fraction increases monotonically with heat flux. At 6 s CHF occurs and the heat transfer mechanism switches to film boiling. The transition takes about 1 s. At 10 s the power begins to decrease. The void fraction decreases while the impact rate remains constant. At 16 s the Leidenfrost point (8 W/cm^2) is reached and the void fraction presents a change in the slope.

The interfacial impact rate has a linear dependence with heat flux in the nucleate boiling region.

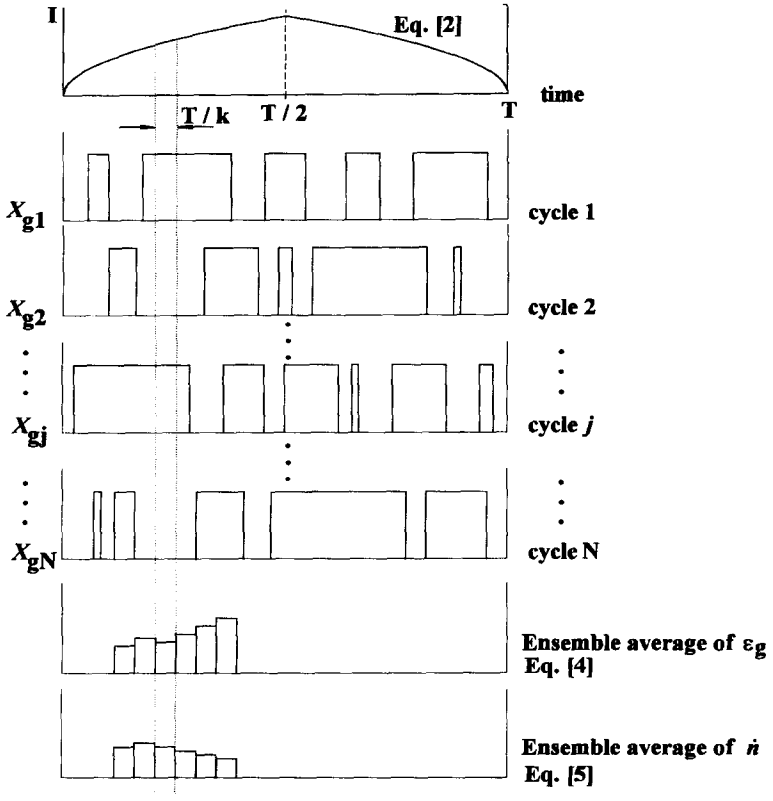

Figure 3. Ensemble average of N identical power cycles.

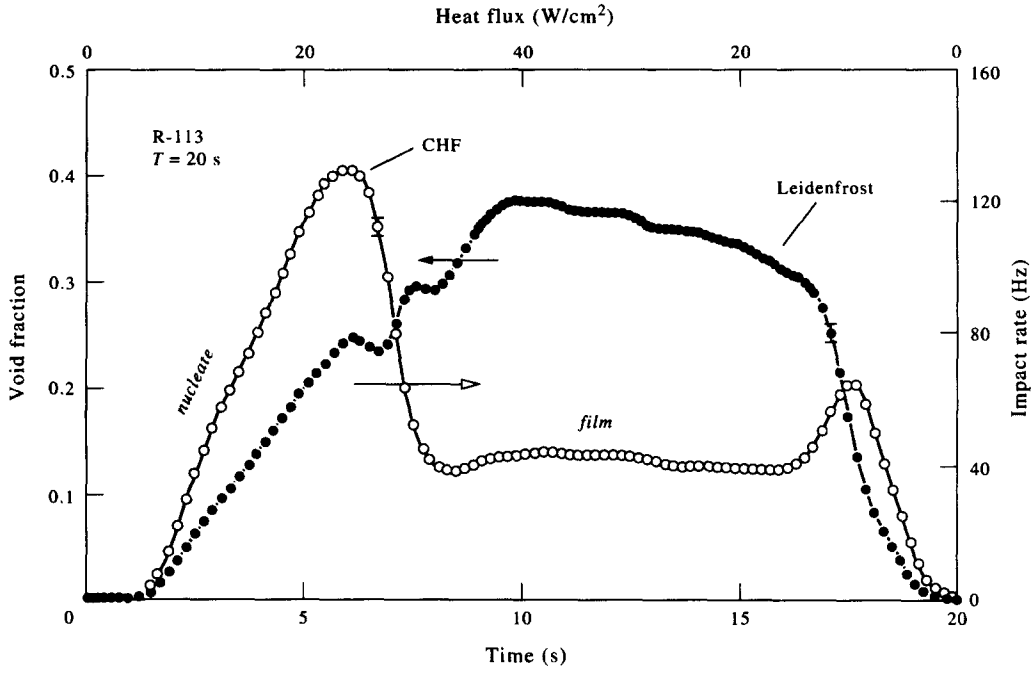

Figure 4. Time evolution of impact rate and void fraction for R-113 at $T = 20$ s. Error bars correspond to the maximum statistical errors.

In film boiling the impact rate remains almost constant with power around 40 impacts per second. An interesting peak of the impact rate can be observed during the Leidenfrost transition.

Figure 5 shows the dynamic evolution for an oscillation period $T = 2$ s. In this case the inertia of the heater is of the order of the period of oscillation. In the CHF the void fraction first decreases and then recovers in stable film boiling while the impact rate experiences a substantial drop. Interestingly, the value of the CHF is the same on both frequencies. On the other hand, the

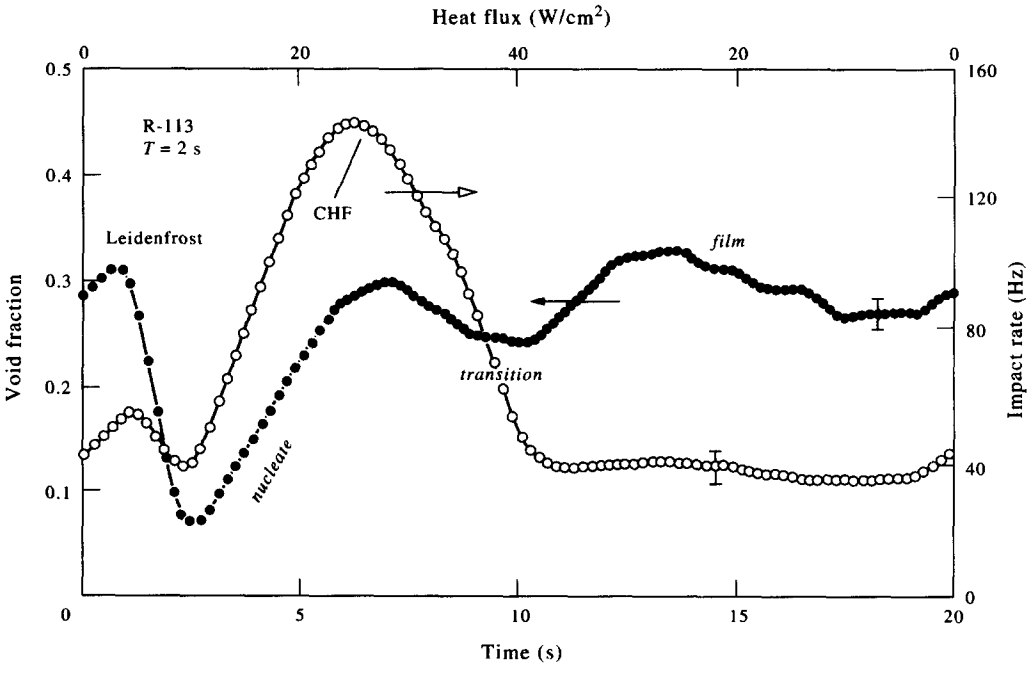

Figure 5. Time evolution of impact and void fraction for R-113 at $T = 2$ s. Error bars correspond to the maximum statistical error.

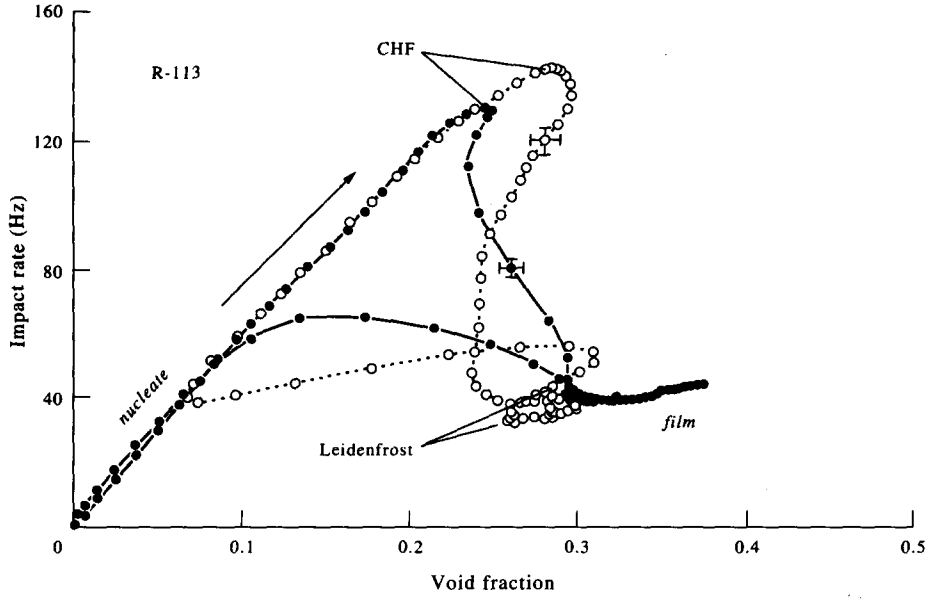

Figure 6. Trajectories in the void fraction–impact rate plane for R-113. Open and solid symbols correspond, respectively, to 0.5 and 0.05 Hz.

Leidenfrost point can be recognized by the peak of the impact rate at 0.1 s after the beginning of the cycle. There is a clear shift in the occurence of the transition, caused by the thermal delay of the heater.

In figure 6 results of both periods are plotted in the impact rate–void fraction plane. The trajectories in nucleate and film boiling are essentially the same, except for the different void fraction values reached in the CHF and Leidenfrost points. On the contrary, the transitions clearly show different paths.

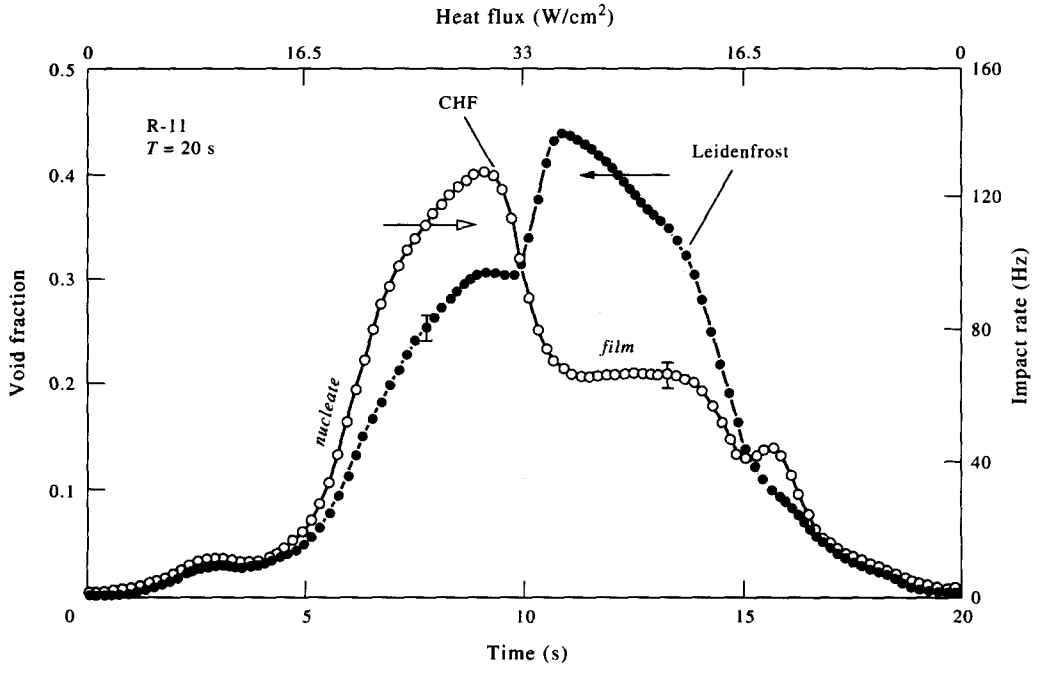

Figure 7. Time evolution of impact rate and void fraction for R-11 at $T = 20$ s.

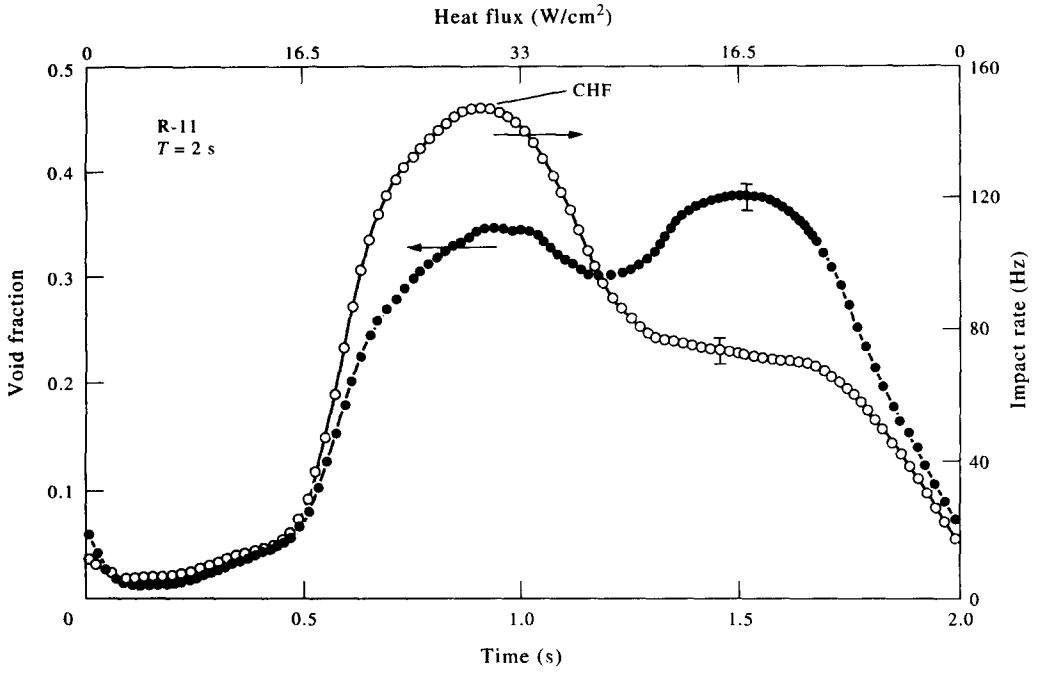

Figure 8. Time evolution of impact rate and void fraction for R-11 at $T = 2$ s.

Experiments in R-11

In figure 7 the time evolution in R-11 of the of the void fraction and impact rate for $T = 20$ s are shown. The heater resistance was 26 mΩ and the maximum current in each cycle was 230 A. This maximum current was limited by freon decomposition and infrared saturation of the optical probe. CHF appeared at 220 A corresponding to 30 W/cm^2, and rewetting occurs at 11 W/cm^2. By comparison with the correspondent evolution in R-113, (figure 4) it can be observed that the overall shape is similar, although in figure 8 (R-11) the curves are more squeezed to the center because both transitions are closer to each other than in R-113.

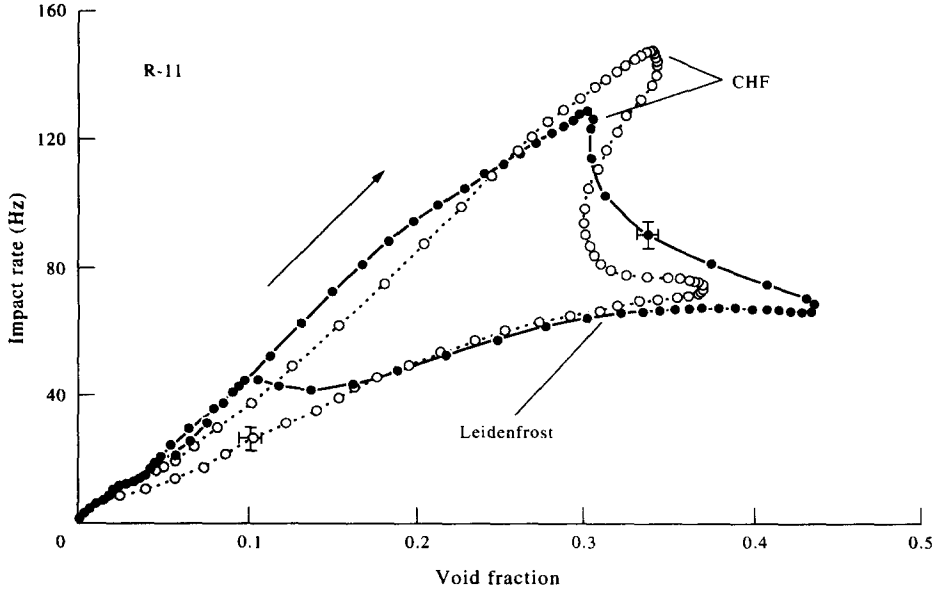

Figure 9. Trajectories in the void fraction–impact rate plane for R-11. Open and solid symbols correspond, respectively, to 0.5 and 0.05 Hz.

In figure 8 the evolution in R-11 for a period of 2 s is shown. A time shift of 0.25 s with respect to the 20 s oscillation is observed. The peak in the void fraction corresponding to the Leidenfrost point, which appeared in R-113, is not present in R-11. The value of the CHF is about the same for both frequencies. The results for both periods plotted in the void fraction–impact rate plane can be seen in figure 9. R-11 shows the same trend observed in R-113: the void fraction and impact rate reached in the CHF are higher in the faster oscillation.

Experiments in water

The experiments in water were performed using a heater of $R_h = 35\ m\Omega$ at 120°C. Independent runs were carried out for each frequency, and repetitivity verified. The current was oscillated from 100 to 600 A, the maximum being limited by the heater integrity. The onset of nucleate boiling appeared at 150 A.

The critical heat flux was found at 170 W/cm^2, corresponding to a current of 570 A. This value appears to be quite high compared with the values found in the bibliography for large heaters (about 110 W/cm^2). Haramura & Katto (1983) reported measurements performed on a small horizontal disk (10 mm diameter) in saturated water, with a range of values of 130–170 W/cm^2. They generalize the results with a model of CHF, based on the inflow from the perimeter of the heater, defining a factor $1 + k$ to take into account this effect (k increases with perimeter/area). In the experiments of Harmura & Katto, the value of perimeter/area of the heater is 4 cm^{-1} while in our heater this value is 6 cm^{-1}. This means that in our heater the CHF should be higher than that of Haramura & Katto. Also in the experiments presented by Lienhard *et al.* (1973) for finite size horizontal heaters, the peak heat flux is shown to increase when the heaters are smaller. They found CHF values of up to two times higher than those corresponding to infinite heaters using three different liquids.

In figure 10 the evolution of void fraction and impact rate for a period $T = 20$ s is shown. The averaging process was carried out partitioning the cycle in 100 time intervals. The transition from nucleate to film boiling is not as clear as in freons. The impact rate has a peak at about 80 W/cm^2. This peak in the impact rate is due to the hydrodynamic transition in nucleate boiling from the isolated bubbles regime to the "vapor mushrooms" regime (Moissis & Berenson 1963), which leads to a smaller impact rate because the bubbles are bigger.

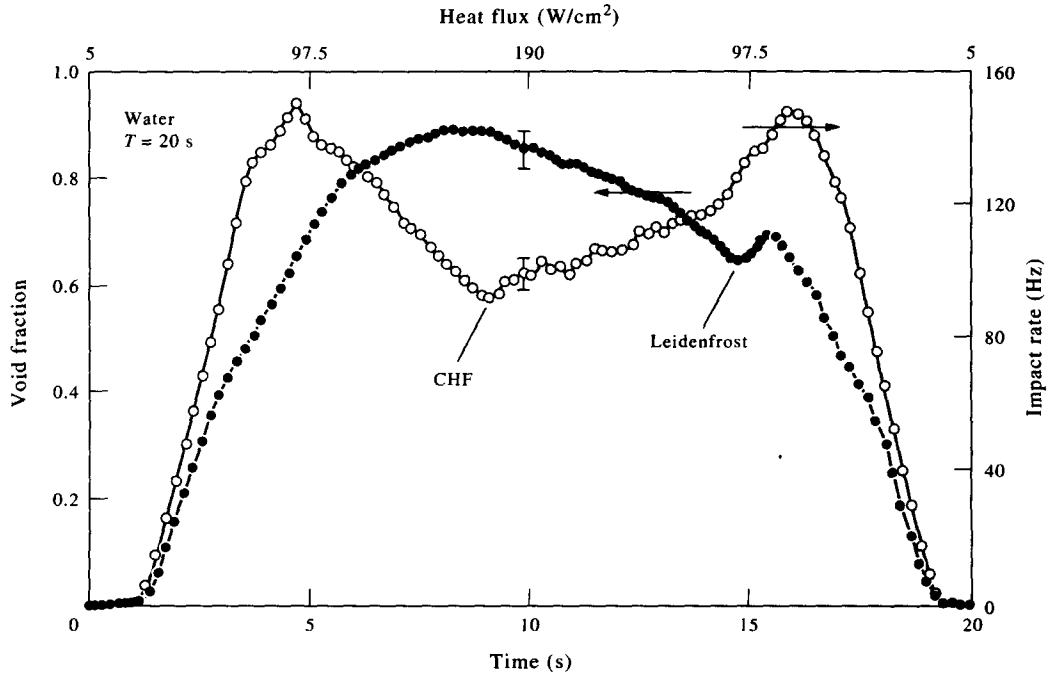

Figure 10. Time evolution of impact rate and void fraction for water at $T = 20$ s.

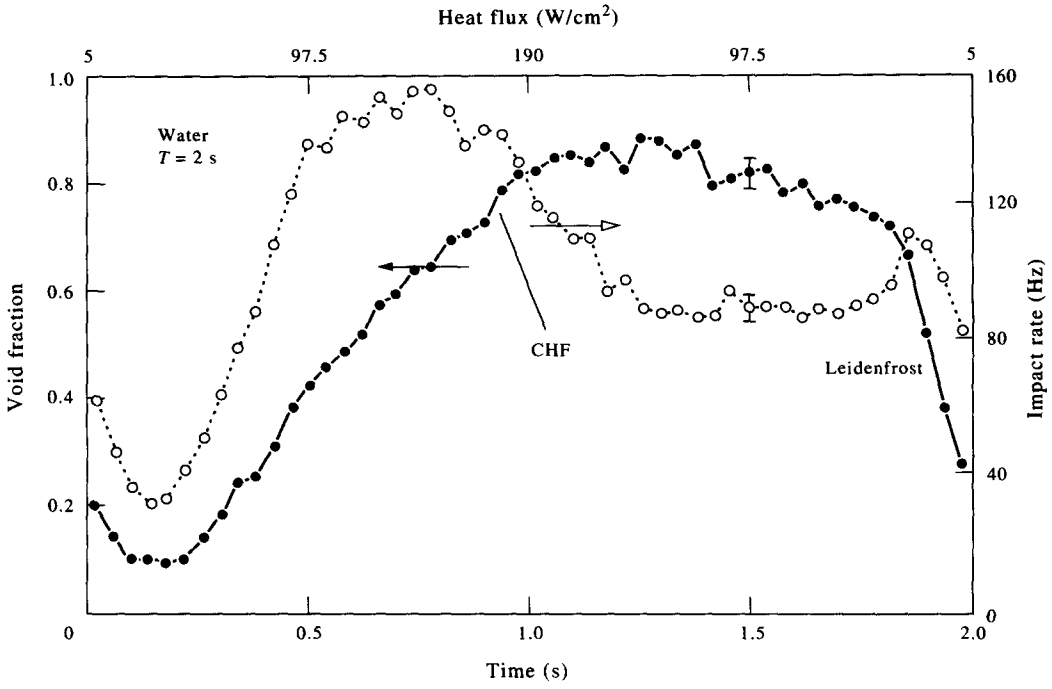

Figure 11. Time evolution of impact rate and void fraction for water at $T = 2$ s.

The CHF occurs at about 9 s. It is recognized by a maximum of the void fraction and a minimum of the impact rate. The smoothness of the transition suggests that the acting mechanism is of liquid film dryout type, in agreement with the hypothesis made by Haramura & Katto (1983). On the other hand, the transition from film to nucleate boiling is characterized by a peak in the void fraction caused by an increase in the heat flux due to the drop of the heater temperature and consequently of the heater resistance. This effect is not important in freons because the temperature change in the Leidenfrost transition is small and the heat flux only increases about 5%.

The evolution for $T = 2$ s is shown in figure 11. The ensemble average was made taking 50 time intervals. The time shift due to the heater inertia is about 0.3 s.

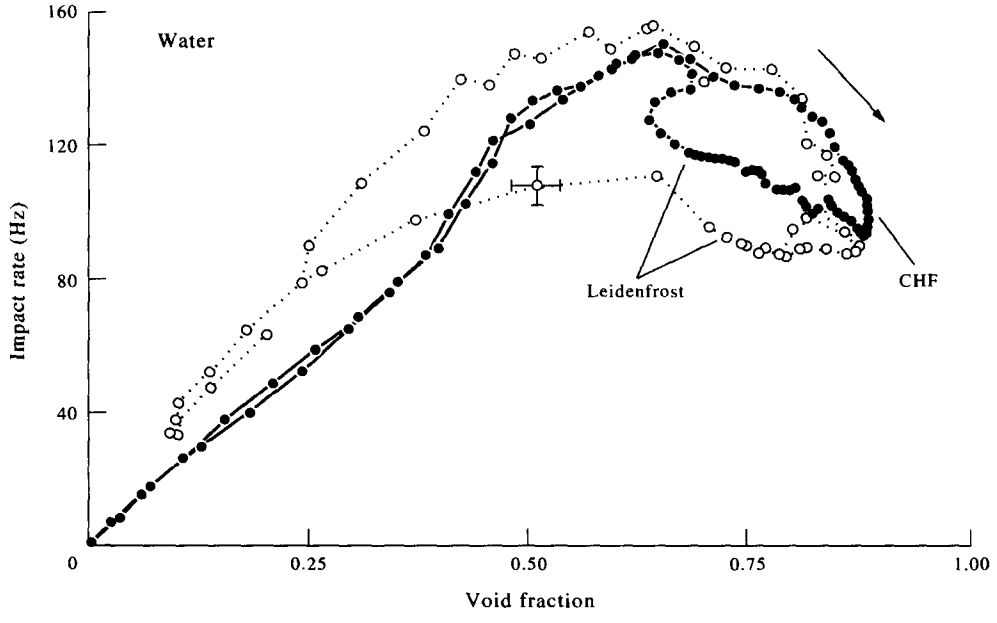

Figure 12. Trajectories in the void fraction–impact rate plane for water. Open and solid symbols correspond, respectively, to 0.5 and 0.05 Hz.

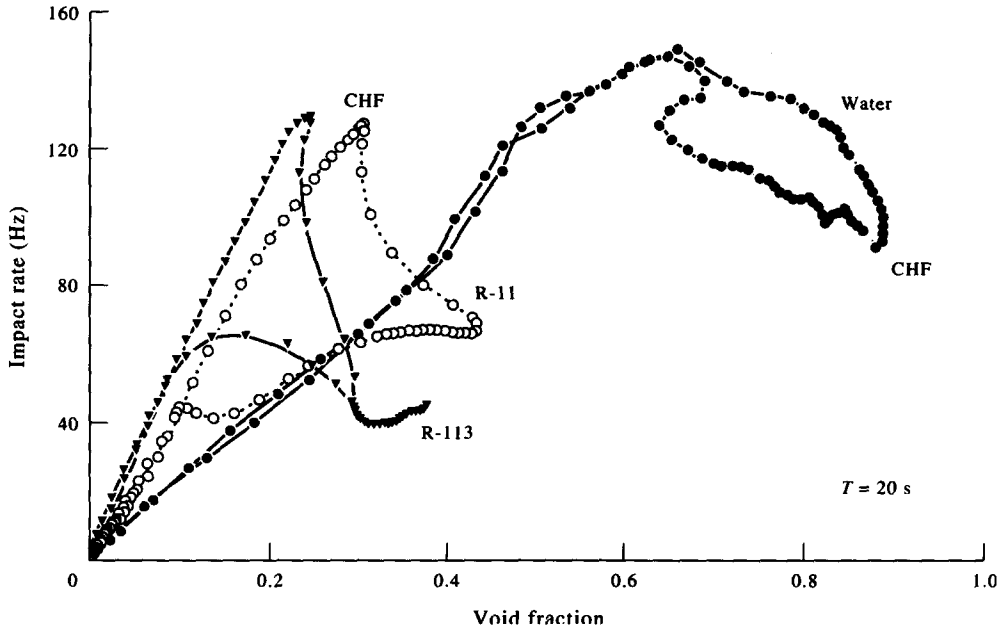

Figure 13. Trajectories of the three fluids for $T = 20$ s.

In figure 12 the results are shown in the void fraction–impact rate plane. As in freons, when the period is large, the path is the same in nucleate boiling either increasing or decreasing power. On the contrary, in film boiling the path is different when the power is increasing or decreasing. The same behavior is observed when the oscillation frequency is higher.

In figure 13 the results of the three fluids in the void fraction–impact rate plane are shown for a power oscillation of a 20 s period. It is interesting to observe the similarity of the freon cycles, in contrast with the cycle in water. Figure 14 presents the same plot normalized with the maximum values of void fraction and impact rate.

Video tape observations were performed during the experiments to complete the picture of the study. Particularly interesting is the film boiling regime where bubbles are seen to detach irregularly from the film. The latter is a consequence of the size of the heater, which is smaller than the "most

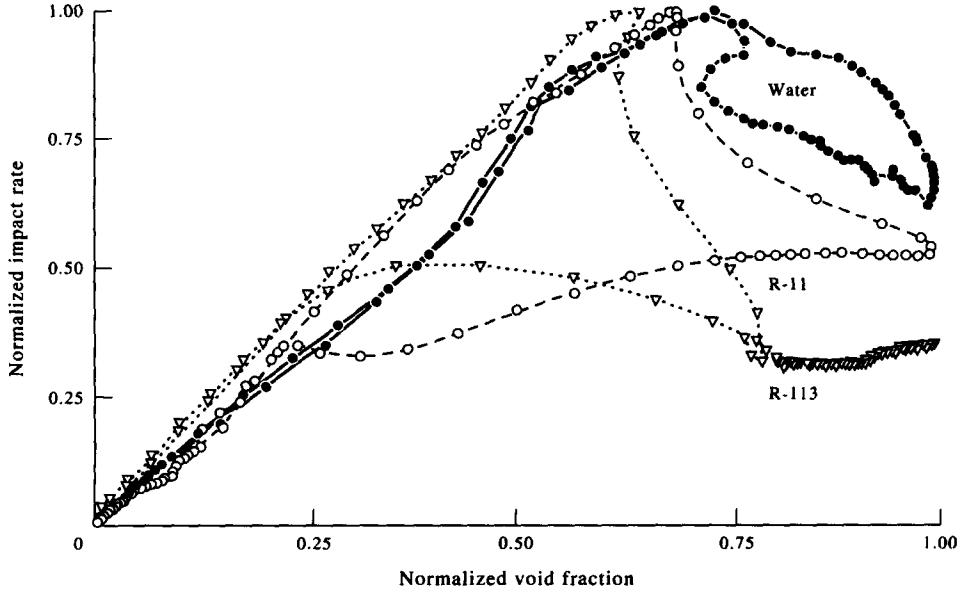

Figure 14. Figure 13 normalized with the maximum values of void fraction and impact rate.

dangerous" Taylor wavelength:

$$\lambda_T = 2\pi \sqrt{\frac{3\sigma}{\mathbf{g}(\rho_L - \rho_G)}} \quad [8]$$

λ_T = the Taylor "most dangerous" wavelength (m)
ρ_L = density of liquid
ρ_G = density of gas

which gives 12 mm for freons and 27 mm for water. Therefore, the Taylor wavelength is larger than the heater width for both freons and water (this means that the heater is small in all liquids).

It is interesting to note that in nucleate boiling the bubbles detach from many nucleation sites both in freons and water. However, close to CHF two vapor mushrooms are formed over the heater in the water case, while in freons the many bubbles regime is observed in all nucleate boiling regimes.

CONCLUSIONS

A method for measuring fast temporal variations of the void fraction and the interfacial impact rate is presented. Ensemble averages of the data have been carried out to obtain time evolution of the void fraction and the interfacial impact rate at the probe tip located in a transient two-phase field.

A dynamical study of the local two-phase flow parameters near a horizontal heater in nucleate and film pool boiling has been performed. R-113, R-11 and water have been used as working fluids, finding important differences between the behavior of the freons and the water at the boiling crises. The critical heat flux transition in freons is associated with a sudden transition in the impact rate and the void fraction, which supports the theory of a hydrodynamic instability (Zuber 1959, Lienhard & Dhir 1973, Carrica & Clausse 1992). On the other hand, the experiments in water suggest the existence of two transitions: a hydrodynamic transition from the bubbling regime to the "mushroom" regime (Moissis & Berenson 1963); and a liquid film dryout type of CHF, in agreement with the theory of Haramura & Katto (1983). It should be mentioned though, that the experimental results do not confirm any of the theories. They are in agreement with the suggested models, but they do not preclude other interpretations which may arise from other different models.

Moreover, the difference in maximum void fractions between freons and water is probably due to the differences in contact angles—2–5° in freons (Tong *et al.* 1990) and one order of magnitude larger in water (Liaw & Dhir 1989)—the results of the present investigation support the conclusion reached by Dhir & Liaw (1989) that different mechanisms determine the CHF, depending on the surface wettability. The results obtained in the present study can be of great value for testing against theoretical models of boiling heat transfer and crises.

Acknowledgement—The authors acknowledge Daniel Mateos for his careful construction of the experimental facilities.

REFERENCES

AID S.A. 1977 *Service Manual Probe No. 7915. DISA Inf. Department, Meylan, France.*

ANNUNZIATO, M., GIAMMARTINI, S., PRESAGHI, M. & SICA, M. 1987 Void fraction measurement with optical probe system. *European Two-phase Flow Group Meeting*, Trondheim, Norway.

BONETTO, F., CLAUSSE, A. & CONVERTI, J. 1992 Two-phase flow in the localized boiling field adjacent to a heated wall. *Int. J. Heat Mass Trans.* **36,** 1367–1379.

CARRICA, P. M. & CLAUSSE, A. 1994 A mathematical description of the critical heat flux as a nonlinear dynamic instability. *Latinam. J. Appl. Res.* **24,** 77–87.

CARRICA, P. M., MORAGA, F. & CLAUSSE, A. 1992 Measurements of void fraction spatial distributions in pool boiling. *Int. Comm. Heat Mass Trans.* **19,** 499–505.

CARRICA, P. M., ACHTERBERG, J., TAGLIALAVORE, E. & LEONARDI, S. 1993 A conductive aquisition system for the local phase indication function. CNEA-CAB 93/012 Technical Report.

CARTELLIER, A. 1990 Optical probes for void fraction measurements: characterization of performance. *Rev. Sci. Instrum.* **61,** 874–886.

CARTELLIER, A. & ACHARD, J. L. 1991 Local phase detection probes in fluid/fluid two-phase flows. *Rev. Sci. Instrum.* **62,** 279–303.

DHIR, V. K. 1991 Nucleate and transition boiling heat transfer during pool and external flow conditions. *Int. J. Heat Fluid Flow* **12,** 290–313.

DHIR, V. K. & LIAW, S. P. 1989 Framework for a unified model for nucleate and transition pool boiling. *ASME J. Heat Transfer* **111,** 739–746.

GALAUP, J. P. 1975 Thesis presented at the Université Scientifique et Medicale de Grenoble et L'Institut National Polytechnique de Grenoble.

HARAMURA, Y. & KATTO, Y. 1983 A new hydrodynamic model of critical heat flux applicable widely to both pool and forced convection boiling on submerged bodies in saturated liquids. *Int. J. Heat Mass Transfer* **26,** 389–399.

HINZE, J. O. 1975 *Turbulence.* McGraw–Hill, New York.

IIDA, Y. & KOBAYASHI, K. 1969 An experimental investigation on the mechanism of pool boiling phenomena by a probe method. *4th Int. Heat Transfer Conference*, Vol. 5, B1.3.

KALININ, E. K. BERLIN, I. I. & KOSTIUK, V. V. 1975 Film boiling heat transfer. *Adv. Heat Transfer* **11,** 51–197.

KALININ, E. K. BERLIN, I. I. & KOSTIUK, V. V. 1987 Transition boiling heat transfer. *Adv. Heat Transfer* **18,** 241–320

LIAW, S. P. & DHIR, V. K. 1989 Void fraction measurements during saturated pool boiling on partially wetted vertical surfaces. *ASME J. Heat Transfer* **111,** 731–738.

LIENHARD, J., DHIR, V. K. & RIHERD, D. M. 1973 Peak pool boiling heat flux measurements on finite horizontal plates. *ASME J. Heat Transfer* **95,** 477–482.

LIENHARD, J. 1988 Things we don't know about boiling heat transfer. *Int. Comm. Heat Mass Transfer* **15,** 401–428.

MOISSIS, R. & BERENSON, P. J. 1963 On the hydrodynamic transitions in nucleate boiling. *Trans. ASME J. Heat Transfer* **85,** 221–229.

SHOJI, M. 1992 Experimental verification of macrolayer evaportion model. *The Engineering Foundation Conference on Pool and External Flow Boiling* (Edited by DHIR, V. K. & BERGLES, A. E.) pp. 237–242.

TONG, W., BAR-COHEN, A., SIMON, T. W. & YOU, S. M. 1990 Contact angle effects on boiling incipience of highly-wetting liquids. *Int. J. Heat Mass Transfer* **33,** 91–103.

VAN DER WELLE, L. 1985 Void fraction, bubble velocity and bubble size in two-phase flow. *Int. J. Multiphase Flow* **11,** 317–345.

VAN STRALEN, S. & COLE, R. 1979 *Boiling Phenomena*, pp. 155–196. Hemisphere, New York.

ZUBER, N. 1959 Hydrodynamic aspects of boiling heat transfer. AEC Report, AECU-4439.

APPENDIX

Measurement of Heater Thermal Inertia

Quenching experiments were carried out in freon 113 to measure the thermal relaxation time of the heater. The heater is set in film boiling at 450°C for 6 s and then the power supply is suddenly disconnected for 9 s. In order to have a sharp cut of the current to the heater the power-out relay of the DC power supply was controlled. The time needed by the departing bubbles to reach the probe was calculated in about 0.02–0.03 s (based on the velocities observed with video equipment).

In figure A1 (overleaf) the ensemble average of the void fraction and the interfacial impact rate over 200 cycles are shown. It can be seen that once the power is switched off the void fraction decreases, reaching a minimum about 0.25 s later. At this moment the Leidenfrost point is reached and the film breaks up into small bubbles, increasing the interfacial impact rate up to a maximum where the transition region ends and nucleate boiling becomes stable. Finally, in the last stage the heater cools down by natural convection without boiling. The cooling time from 450 to 150°C was about 0.3 s and the total time until boiling stops is about 0.5 s.

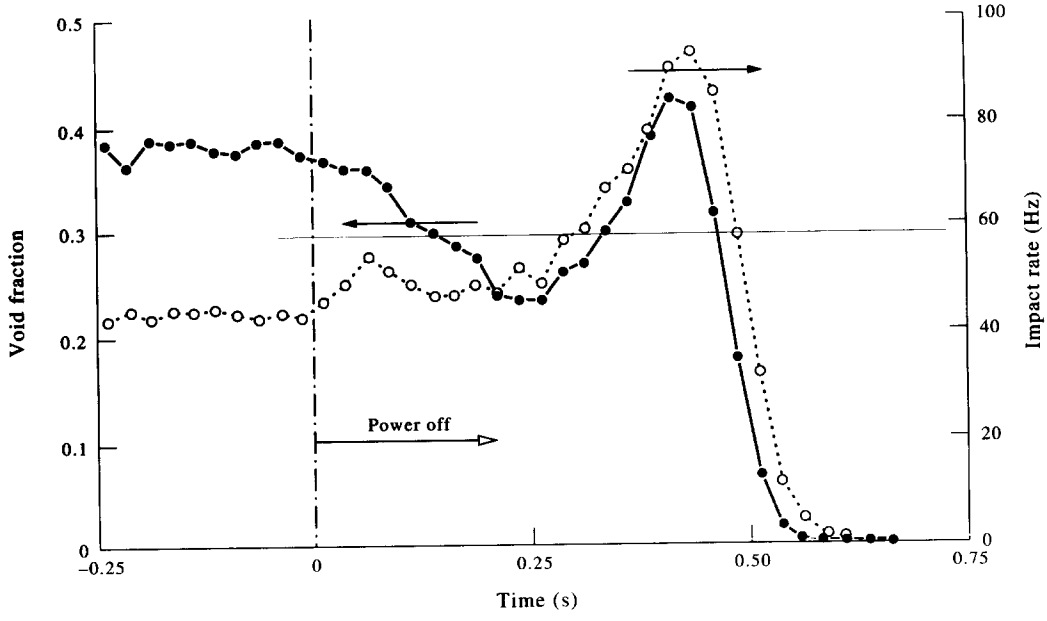

Figure A1. Time evolution of the two-phase parameters after a sudden power drop.